



CHORUS

This is the accepted manuscript made available via CHORUS. The article has been published as:

Polarization switching in the $\text{PbMg}_{\{1/3\}}\text{Nb}_{\{2/3\}}\text{O}_{\{3\}}$ relaxor ferroelectric: An atomistic effective Hamiltonian study

Sergey Prosandeev, Bin Xu, and L. Bellaiche

Phys. Rev. B **98**, 024105 — Published 26 July 2018

DOI: [10.1103/PhysRevB.98.024105](https://doi.org/10.1103/PhysRevB.98.024105)

Polarization switching in $\text{PbMg}_{1/3}\text{Nb}_{2/3}\text{O}_3$ relaxor ferroelectric: an atomistic effective Hamiltonian study

Sergey Prosandeev^{1,2}, Bin Xu¹ and L. Bellaiche¹

¹*Physics Department and Institute for Nanoscience and Engineering,
University of Arkansas, Fayetteville, Arkansas 72701, USA*

²*Institute of Physics and Physics Department of Southern
Federal University, Rostov-na-Donu 344090, Russia*

Abstract

An atomistic effective Hamiltonian technique is employed to investigate the polarization switching mechanism of the (metastable but long-living) ferroelectric state of $\text{PbMg}_{1/3}\text{Nb}_{2/3}\text{O}_3$ relaxor ferroelectric, resulting from the application of a *dc* electric field along the $[\bar{1}\bar{1}\bar{1}]$ direction – that is, opposite to the initial polarization. It is predicted that such switching is of inhomogeneous type. It involves the creation of intermediate short-range-ordered, relaxor-like phases in-between long-range ordered states inside which an infinite cluster exists and have dipoles being near either the initial polarization direction (for shorter times) or the field’s direction (for longer times). In contrast, dipoles belonging to finite clusters or being isolated can deviate away from $[111]$ and $[\bar{1}\bar{1}\bar{1}]$, and, in fact, rotate in average from $[111]$ to $[\bar{1}\bar{1}\bar{1}]$ when time increases. Such rotations govern the reversal of the polarization from $[111]$ to $[\bar{1}\bar{1}\bar{1}]$ occurring within the intermediate relaxor-like states’ region, while always resulting in the overall cancellation of any Cartesian component of the polarization that is perpendicular to $[111]$. These rotations occurring at the atomic scale also naturally imply that some fundamental assumptions of the original nucleation-limited-switching (NLS) model are not valid, despite the fact that we numerically further find that the whole temporal behavior of the macroscopic polarization can be well fitted by the general formula associated with NLS. In other words, we have stumbled into a novel switching or at least to a switching that should be denoted as a generalized NLS model. Finally, three different electric field regimes are predicted, with each of them having its own dependency of the switching time on the magnitude of the applied electric field and only one of them obeying the Merz’s law. The existence of these three regimes is explained in terms of specific microscopic features.

I. INTRODUCTION

Switching of the electrical polarization under an external electric field has been investigated in ferroelectric compounds for many years, because of its fundamental interest but also for technological applications¹⁻¹⁷. In particular, a recent study showed that a specific type of polarization switching can lead to solid-state synapses and is thus promising for designing future-brain-inspired computers¹⁸. Such particular type is inhomogeneous in nature and is termed the nucleation-limited-switching (NLS) model. It assumes that different areas of the film adopt different switching dynamics, with a limited propagation of the domain walls separating these areas from the host matrix^{4-7,15}. Another type of inhomogeneous switching of the polarization has been proposed and documented in the literature¹⁹⁻²¹, that is the so-called Kolmogorov-Avrami-Ishibashi (KAI) model. It consists of inhomogeneous nucleation of reversed domains too but with significant (i.e., “unlimited”) domain-wall motions. In addition to the inhomogeneous NLS and KAI models, *homogeneous*-types of polarization switching (that is without nucleation of domains) have also been reported in some ferroelectric systems⁸⁻¹¹. One can envision two different types of homogeneous switching when applying an external electric field that is opposed to the initial polarization, namely (1) the polarization of a monodomain is first continuously reduced in magnitude with no change of direction, until fully vanishing and then reverting its direction to become parallel to the field²²; or (2) the polarization of a monodomain rather progressively *rotates* away from its initial direction towards the direction of the electric field²³.

It may be provocative to wonder if novel types of polarization switching have been overlooked in the past, considering the aforementioned activities. However, to the best of our knowledge, polarization switching has been poorly investigated to date in a specific subclass of ferroelectrics, and surprises may thus be in store for them. This subclass is formed by ferroelectric relaxors, that are known to exhibit unusual properties. For instance, their dielectric response-*versus*-temperature function exhibits a peak, that is not only unusually broad but is also strongly dependent on the frequency of the applied *ac* electric field, while they remain macroscopically non-polar down to 0K^{24,25}. Such unusual behaviors are often ascribed to the existence of so-called polar nanoregions (PNRs) inside which dipoles are parallel to each other²⁶⁻³⁰, with the direction of such dipoles differing between various PNRs such that to provide a zero macroscopic polarization. Interestingly, the application of *dc* electric fields to

relaxor ferroelectrics can have dramatic consequences on their local structure and polarization. For example, applying, at low temperature, a large enough dc electric field along the pseudo-cubic $[111]$ direction in the lead magnesium niobate $\text{PbMg}_{1/3}\text{Nb}_{2/3}\text{O}_3$ (PMN) prototype relaxor ferroelectric results in a first-order transition from a relaxor state to a regular ferroelectric state having a now-finite macroscopic polarization lying along the pseudo-cubic $[111]$ direction³¹⁻³³. Such latter ferroelectric state even persists, rather than transforms back to the relaxor phase, when removing the applied electric field at low temperature³⁴. One may ask what will happen to the spontaneous polarization of this (metastable) ferroelectric state when applying a dc electric field that is opposed to such polarization. Will the switching be homogeneous or inhomogeneous? If it is the latter, many questions arise. For instance, will it pass through a relaxor-kind of state consisting of PNRs having different direction of the polarization? Will it be of NLS or KAI type or can it even be a novel kind of inhomogeneous switching? Does the switching type depend on the magnitude of the applied electric field, as recently found in the so-called T-phase of BiFeO_3 ¹⁷ when identifying three different fields regimes – each adopting its own Merz’s law³⁵?

The goal of this manuscript is to address such questions by performing atomistic simulations. As we are going to see below, the polarization-*versus*-time function obeys rather accurately the behavior predicted by the NLS model. However, local aspects associated with the switching mechanism differ from some basic assumptions of the NLS model, implying that either a new name has to be given for the presently discovered switching or the wording “generalized NLS model” should be adopted. As a matter of fact, the switching mechanism is found here to (i) involve long-ranged polar states inside which the so-called infinite cluster (that is inherent to percolation theory) occurs and whose strength dramatically depends on time, as well as (ii) intermediate relaxor-like state inside which the infinite cluster has been destroyed. Moreover, the dipoles of the infinite cluster can only lie near $[111]$ (at small times) or $[\bar{1}\bar{1}\bar{1}]$ (at large times), while the dipoles that do *not* belong to this infinite cluster adopt rotations away from $[111]$ that are primordial in the reversal of the polarization (that occurs within the relaxor-like states). *These rotations are not included in the standard NLS model.* Finally, varying the magnitude of the applied electric field still yields a temporal dependency of the macroscopic polarization that is well described by the NLS model, but for which the characteristic switching time adopts three different behaviors with such magnitude. These three regimes are related to specific local features inherent to the infinite cluster, such that

the time-dependency of its polarization or the time-dependency of its strength. Such dependencies result in only one out of these three regimes obeying the conventional Merz's law³⁵.

This article is organized as follows. Section II provides details about the methods used, while Section III reports predictions and their analyses. Finally, Section IV summarizes the main findings.

II. METHODS

Here, molecular dynamics (MD) calculations³⁶ are conducted on an $18 \times 18 \times 18$ disordered periodic configuration of PMN, by using the effective Hamiltonian developed in Ref. [37]. This effective Hamiltonian has the following degrees of freedom: (1) the local modes in each 5-atom cell, \mathbf{u}_i , which are directly proportional to local dipole moments; (2) the homogeneous strain, $\boldsymbol{\eta}_H$; and (3) dimensionless vectors, \mathbf{v}_i , that are related to the local inhomogeneous strain existing inside each 5-atom cell i ³⁸. This effective Hamiltonian has been recently shown to reproduce the existence of several specific temperatures inherent to relaxor systems, such as the Burns temperature, as well as, the so-called T^* and depolarizing temperatures³⁷. It was also put in use to predict that such temperatures are strongly affected by short-range-order chemical ordering between the Mg and Nb ions in the B-sublattice of PMN³⁹, and to explain the origin of its relaxor nature from a subtle competition between (i) random electric fields arising from the alloying of Mg and Nb ions in this B-sublattice; (ii) the simultaneous condensation of several off-center k points as a result of antiferroelectric-like interactions between lead-centered dipoles; and (iii) ferroelectric-like interactions³⁷. Such effective Hamiltonian also revealed the existence of polar nanoregions (PNRs) in the relaxor state of PMN³⁷.

During our MD computations, the following equations of motion are solved:

$$\frac{\partial E_{tot}}{\partial \mathbf{q}_i} = -m_q \frac{\partial^2 \mathbf{q}_i}{\partial t^2} \quad (1)$$

where E_{tot} is the internal energy provided by the effective Hamiltonian, \mathbf{q}_i represents the aforementioned degrees of freedom in the unit cell i (note that, for the homogeneous strain, \mathbf{q}_i is in fact independent of the i index) and m_q is the mass associated with these degrees of freedom. Technically, the mass of the local modes is selected such as to reproduce experi-

mental phonon frequencies at some temperatures^{40–44}, and the masses of the homogeneous and inhomogeneous strains are chosen to be rather large in order to avoid generating additional frequencies of the order of cm^{-1} . Technically, the MD time step is chosen to be 0.5 fs. The initial generalized velocities $\dot{\mathbf{q}}_i$ were selected randomly, but with the requirements that the average kinetic energies per primitive cell related to the generalized velocities $\dot{\mathbf{u}}_i$ and $\dot{\mathbf{v}}_i$ are each equal to $\frac{3}{2}k_B T$, where k_B is the Boltzmann constant and T is temperature – which, in the present study, amounts to 10 K. We also first pole our PMN sample by applying a *dc* electric field of magnitude $5 \times 10^8 \text{V/m}$ along the [111] direction and equilibrate it by performing Monte Carlo calculations³⁷. We then remove this field and equilibrate the system again, which results in the system retaining its ferroelectric state (rather than coming back to a relaxor phase), as consistent with experiments³⁴. The corresponding equilibrated polar structure is then subject to a *dc* electric field applied along the $[\bar{1}\bar{1}\bar{1}]$ direction (that is, opposed to the initial polarization) within the MD simulations. In the present study, we choose different magnitude of such latter *dc* electric field, in order to reveal and understand its effect on polarization switching in PMN. Note that we numerically found⁴⁵ that, quantitatively, the field’s magnitudes employed in our simulations are about 22 times larger than the measured ones³³, which is typical for atomistic simulations^{16,46,47}.

III. RESULTS

Figure 1a shows the temporal dependence of the $\langle \mathbf{u} \rangle$ supercell average of the local mode vectors (such average is directly proportional to the electrical polarization) for three different field’s magnitudes, namely $3.5 \times 10^7 \text{V/m}$, $8.0 \times 10^7 \text{V/m}$ and $2.0 \times 10^8 \text{V/m}$, respectively (note that, as we will see towards the end of this article, each of those fields is representative of a particular regime). Such supercell average is shown in the (x', y', z') basis for which the x' , y' and z' -axes are along the pseudo-cubic $[1\bar{1}0]$, $[11\bar{2}]$ and $[111]$ pseudo-cubic directions, respectively. Only the z' -component of the polarization is finite, since both the x' - and y' -components are found to be negligible for any time and for any applied electric field (and are thus not shown in Fig. 1a for clarity). As a result, the presently studied switching mechanism does *not* involve a continuous rotation of the spontaneous polarization from its initial direction to the field’s direction, which contrasts with the mechanism invoked in Ref.²³. Moreover, the projection of the supercell average of the local mode vectors on the

pseudo-cubic [111] direction (to be denoted as $\langle u_{z'} \rangle$) is first positive and decreases with time, until passing through a zero value and becoming negative as time further evolves, which is representative of a switching of the polarization from [111] to $[\bar{1}\bar{1}\bar{1}]$ under the influence of the electric field. The time at which $\langle u_{z'} \rangle$ vanishes will be denoted here as t_0 and represents the switching time. Figure 1a further indicates that t_0 is rather sensitive to the magnitude of the applied electric field, and decreases when this magnitude increases. Note that the inset of Fig. 1a also displays the $\langle |u| \rangle$ average *magnitude* of the individual local modes as a function of time and reveals that such magnitude is rather unchanged with time in the case of these three fields (even for times close to t_0). As a result, the switching mechanism of PMN is *not* a homogeneous one for which the local dipoles all simply first shrink in magnitude along [111], then all become annihilated at the same time before all lying along $[\bar{1}\bar{1}\bar{1}]$ and increasing their magnitude until reaching saturation.

In order to determine the switching mechanism of the polarization of the polar state of PMN, we employ the theory of percolation⁴⁸. More precisely, we computed the so-called strength of the infinite cluster, P_{inf} , as the relative number of the sites belonging to clusters spreading from one boundary of the supercell to the opposite boundary and inside which the dipoles are parallel to each other within 32 degrees (that is, the angle between dipoles belonging to such clusters have a cosine equal or greater than 0.85). A value of +1 for P_{inf} therefore indicates that *all* sites of the supercell have dipoles being oriented along the same direction within 32 degrees, while a zero value is indicative that such infinite cluster does not exist. A value of 0.5 represents the case of 50% of the sites of the whole supercell belonging to the infinite cluster. We also calculated the percolation cluster size, $\langle s \rangle$, as:

$$\langle s \rangle = \frac{\sum_i s_i^2}{N} \quad (2)$$

where N is the total number of the sites of the supercell, and s_i is the number of the sites belonging to cluster i inside which the dipoles are parallel to each other within 32 degrees, but *excluding* the dipoles belonging to the infinite cluster. Let us also express words of caution for general readers, namely that the jargon in use in the percolation theory may be thought confusing. For instance, the so-called percolation clusters do *not* percolate within the entire supercell. They are limited in volume, and also include isolated dipoles in our case. The only cluster that is percolating from one side of the supercell to its opposite side is the so-called infinite cluster.

Figures 2a and 2b report P_{inf} and $\langle s \rangle$ as a function of time, respectively, for the three fields used in Figs. 1a. It is informative to realize that, at the initial time, P_{inf} is about 0.7, implying that *not all* the dipoles of the supercell are pointing along the pseudo-cubic [111] direction – therefore characterizing some form of disorder in the ferroelectric phase of PMN, as a result of the distribution of local electric fields originating from the random arrangement between Mg and Nb ions in the B-sublattice. Such disorder arises from sites that either belong to percolation clusters or that have isolated dipoles (all deviating from [111] in direction). Moreover, Figs 1b, 1c and 1d display the averaged local mode that the infinite cluster adopts for these same three fields of $3.5 \times 10^7 \text{V/m}$, $8.0 \times 10^7 \text{V/m}$ and $2.0 \times 10^8 \text{V/m}$, respectively, as a function of time. They indicate, in particular, that the x' and y' components of the polarization of these infinite cluster are basically null at any time and for any field. In other words, the infinite cluster can only have a polarization lying along [111] or $[\bar{1}\bar{1}\bar{1}]$. The contribution of this infinite cluster into the average local mode of the whole system is therefore equal to the product of P_{inf} by the z' -component of the average local mode of the infinite cluster (to be called $u_{inf,z'}$). Such $P_{inf}u_{inf,z'}$ product is further shown in Fig. 1a. It is smaller in magnitude than that of $\langle u_{z'} \rangle$ at any time and for any field, which implies that the dipoles belonging to percolation clusters or being isolated (i.e., being outside the infinite cluster) also always participate in the formation of an overall polarization along the [111] or $[\bar{1}\bar{1}\bar{1}]$ direction. Such latter dipoles have, in fact, directions that can each differ from the [111] and $[\bar{1}\bar{1}\bar{1}]$ directions, as evidenced in Figs. 2c by the fact that the cosine of the angle that the averaged local mode vector of each site belonging to the percolation clusters or being isolated makes with the [111] direction can be different from +1 or -1 (such cosine will be denoted as $\cos(\theta)$, in the following, and has a rather large scattering at the initial time – as representative of the many directions that the sites being outside the infinite cluster can adopt). However, summing all these latter dipoles results in a contribution to the total polarization that is finite only along the [111] or $[\bar{1}\bar{1}\bar{1}]$ direction. In other words, the x' and y' -components of the dipoles belonging to percolation clusters or being isolated always mostly cancel each other, unlike their z' -component. Note that Figs. 2c also shows, by means of a thick red solid curve, the $\cos(\theta)$ averaged over all the sites *not* belonging to the infinite cluster, which is a quantity that will be referred to as $\langle \cos(\theta) \rangle_{not\ inf}$ and that clearly deviates from +1 and -1 at any time and field – therefore characterizing the general tendency of these local dipoles to deviate from [111] and $[\bar{1}\bar{1}\bar{1}]$

directions.

The information reported in Figs 1 and 2 can now fully explain the switching mechanism of the ferroelectric state of PMN. For instance, for all fields, the strength of the infinite cluster first gradually, typically decreases with time until reaching a zero value. During these times, there are therefore more and more sites that leave the infinite cluster, which leads to a decrease of the total polarization along [111] via two combined effects: the contribution of the infinite cluster to the total local mode is reduced (as evidenced by the decrease of $P_{inf}u_{inf,z'}$ with time shown in Fig. 1a), and the dipoles being outside the infinite cluster rotate away from [111] and towards $[\bar{1}\bar{1}\bar{1}]$ (as indicated by the decrease of $\langle \cos(\theta) \rangle_{not\ inf}$ seen in Figs. 2c).

Then, the infinite cluster fully disappears at a time to be denoted as $t_{annih,begin}$, and which amounts to 4.53ps for a field of $3.5 \times 10^7\text{V/m}$, 0.91ps when $E = 8.0 \times 10^7\text{V/m}$, and 0.255ps for the larger field of $2.0 \times 10^8\text{V/m}$. Interestingly, at these precise latter $t_{annih,begin}$ critical times, the disappearance of the infinite cluster is accompanied by the emergence of large percolation clusters with size up to $\langle s \rangle \approx 50$ for the small field of $3.5 \times 10^7\text{V/m}$, $\langle s \rangle \approx 30$ for the intermediate field of $E = 8.0 \times 10^7\text{V/m}$, and $\langle s \rangle \approx 18$ for the larger field of $2.0 \times 10^8\text{V/m}$. The polarization at $t_{annih,begin}$ is slightly positive for any studied field, as a result of the fact that $\langle \cos(\theta) \rangle_{not\ inf}$ is also positive for this time (see Figs. 2c). In other words, at $t_{annih,begin}$, PMN undergoes a transition from a ferroelectric state that is long-ranged ordered (due to the existence of an infinite cluster) to an atypical short-range-like state that is not long-range-ordered anymore but rather owes its slightly positive polarization along [111] to dipoles belonging to percolation clusters and isolated dipoles. When time further increases up to t_0 , (i) the infinite cluster is still non-existent and (ii) the large percolation clusters occurring at $t_{annih,begin}$ then break into smaller percolation clusters, with a minimum size occurring at the t_0 switching time (the percolation clusters' sizes at this minimum are 44, 20 and 5 for fields of $3.5 \times 10^7\text{V/m}$, $8.0 \times 10^7\text{V/m}$, and $2.0 \times 10^8\text{V/m}$, respectively, to be compared with $\langle s \rangle \approx 19$ found in Ref. [37] for the ground state of relaxor phase in PMN at 10 K). The resulting intermediate state can, in fact, be considered as a relaxor phase as evidenced by the existence of polar nanoregions (see inset of the top panel of Fig. 2a) with a vanishing total polarization. Such latter vanishing is consistent with the fact that $\langle \cos(\theta) \rangle_{not\ inf}$ is now null. However, Figs. 2c also reveal that, at $t = t_0$, some sites still have dipoles lying near [111] (their $\cos(\theta)$ is $\simeq +1$) while others prefer to have

their dipoles close to $[\bar{1}\bar{1}\bar{1}]$ (their $\cos(\theta)$ is rather $\simeq -1$). Such features indicate that different regions of the sample have different switching times, which is an essential characteristics of the NLS model (note also that the fact that $\langle \cos(\theta) \rangle_{not\ inf}$ is close to zero near $t = t_0$ does not mean that all dipoles lie in the (111) plane at these times, since there are local $\cos(\theta)$'s that significantly differ from zero even for these times, and as a result, dipoles having finite (positive or negative) components along the pseudo-cubic [111] direction still exist near $t = t_0$).

Further increasing to another critical time that we denote here as $t_{annih,end}$ still leads to the absence of the infinite cluster but the percolation clusters are now gaining in size (see Fig. 2b). For instance, these larger clusters have $\langle s \rangle \approx 85, 50$ and 48 for $3.5 \times 10^7 \text{V/m}$, $8.0 \times 10^7 \text{V/m}$ and $2.0 \times 10^8 \text{V/m}$, respectively. Interestingly, the overall polarization is now along $[\bar{1}\bar{1}\bar{1}]$ because of the continuing overall rotation of the dipoles towards the field's direction (*cf* Fig. 2c). Note that $t_{annih,end}$ is equal to $\approx 5.75\text{ps}, 1.43\text{ps}$ and 0.57ps for E equal to $3.5 \times 10^7 \text{V/m}$, $8.0 \times 10^7 \text{V/m}$ and $2.0 \times 10^8 \text{V/m}$, respectively.

At $t_{annih,end}$, the percolation clusters and isolated dipoles then merge into one another to create a new infinite cluster, therefore making a transition from a short-range-like state to a ferroelectric phase. The polarization of this ferroelectric state is further strengthened along $[\bar{1}\bar{1}\bar{1}]$ because the dipoles belonging to the now-reformed infinite cluster are along such direction (see Figs 1b, 1c and 1d) and because the dipoles belonging to the percolation clusters or being isolated further continue to rotate towards $[\bar{1}\bar{1}\bar{1}]$ (as evidenced by $\langle \cos(\theta) \rangle_{not\ inf}$ becoming closer to -1 in Fig. 2c). Interestingly, we numerically found that the infinite cluster existing just after $t_{annih,end}$ does not contain all the same dipoles than those belonging to the infinite cluster just before $t_{annih,begin}$. In fact, there are only 14% of the dipoles that both belong (1) to the infinite cluster for which $P_{inf} = 0.2$ for a time after $t_{annih,end}$ and (2) to the infinite cluster for which $P_{inf} = 0.2$ too but before $t_{annih,begin}$, when applying the field of $3.5 \times 10^7 \text{V/m}$. These dipoles, before $t_{annih,begin}$ are along the [111] direction, on average, and they are along $[\bar{1}\bar{1}\bar{1}]$ direction just after $t_{annih,end}$.

When increasing the time after $t_{annih,end}$, the strength of this infinite cluster typically continuously increases to about +0.80 for long enough times (at which the switching of the polarization has then been completed), via the further incorporation of dipoles previously belonging to percolation clusters or being isolated. Such strengthening leads to a further overall enhancement of the polarization along the field's direction (since $P_{inf} u_{inf,z'}$ becomes

more and more negative, as revealed by Fig. 1a). Meanwhile, the dipoles being outside the infinite cluster still slightly rotate towards $[\bar{1}\bar{1}\bar{1}]$, which further enhances the overall polarization along such direction (these outside dipoles also still cancel in average their x' and y' components).

Note also that Figs 2a and 2b further show that P_{inf} and $\langle s \rangle$ additionally exhibit some kind of periodic fluctuations in the entire investigated time interval of the simulations, implying that both the infinite cluster and the percolation clusters can “breathe” under the applied dc electric fields. In fact, we numerically found (not shown here) that the Fourier analysis of $\langle s \rangle$, for the three fields depicted in Figs. 1 and 2, possess two strong peaks whose positions indicate the natural frequencies of these breathings: one peak is located near zero frequency with a half-width of about 1 THz, while the other peak is located at 1.6 THz.

Moreover and as aforementioned, the scattering of $\cos(\theta)$ clearly seen in Figs 2c for any field, especially for times ranging between $t_{annih,begin}$ and $t_{annih,end}$, is consistent with one basic ingredient of the NLS model, namely that different regions have different switching times. Moreover, the fact that we did not see any systematic increase of $\langle s \rangle$ with time in Figs. 2b (especially for large fields) is also in-line with another characteristic of the NLS model, i.e. the domain walls of the switched areas have a limited propagation.

To quantitatively check that the NLS model is indeed technically applicable to the switching of the polar state of PMN, Fig. 1a further reports, via red thick solid lines, the fit of the NLS model¹⁵ to our numerical data for the variation of the z' -component of the supercell average of the local mode with time, predicting that:

$$\langle u_{z'}(t) \rangle = \langle u_s \rangle \left[1 - \frac{2 * A}{\pi} \left(\arctan \frac{\log(t) - \log(t_s)}{\log(w)} + \frac{\pi}{2} \right) \right] \quad (3)$$

where $\langle u_s \rangle$ is the initial value of the z' -component of the supercell average of the local mode, and A , t_s and w are some parameters, the values of which are given in Table I. Note, in particular, that A is rather close to 1 for any considered electric field, which implies that t_s is close to t_0 (that is the time at which $\langle u_{z'}(t) \rangle$ vanishes). For instance, for fields of 3.5×10^7 , 8×10^7 and 2×10^8 V/m, t_s is equal to 5.56, 1.29 and 0.46 ps, respectively, to be compared with the corresponding values of 5.20, 1.20, and 0.42 for t_0 . Note that the physical meaning of the parameters entering Eq. (3) are that A is a normalization constant, $\log t_0$ is the central value of the Lorentzian distribution characterizing the switching time,

TABLE I: Parameters of the NLS model fitting our numerical MD data for three different electric fields

$E(\text{V/m})$	3.5×10^7	8×10^7	2×10^8
$\langle u_s \rangle$ (a.u.)	0.085	0.083	0.076
t_s (ps)	5.56	1.29	0.46
w (ps)	1.17	1.28	1.30
A (dimensionless)	1.24	1.16	1.21

and $\log w$ is its half-width at half-maximum.

Figure 1a therefore shows that the fit of the MD data by Eq. (3) is in overall very good for any field, which confirms that the NLS model can be practically applied to describe the polarization switching of the polar phase of PMN.

One should note, however, that other basic ingredients of the NLS model do *not* hold in our discovered switching. For instance, the NLS model assumes that, as soon as one part of an elementary region acquires dipoles being opposed to the initial polarization, the whole elementary region *instantly* switches its polarization along the field direction. Such instantaneous reversal is not observed in our computations, as, e.g., evidenced by the facts that $\cos(\theta)$ of many dipoles belonging to percolation clusters and isolated dipoles rather slowly evolve with time, but also that $\langle \cos(\theta) \rangle_{not\ inf}$ gradually changes with time, as representative of *rotation*, rather than sudden switching, of these dipoles (see Fig. 2c). We are therefore reporting a new type of polarization switching, which should thus been given another name or at least denoted as generalized NLS model (taking into account that the equation of NLS describes well the time evolution of the macroscopic polarization, but fails in reproducing all the atomistic mechanisms associated with the polarization reversal).

Let us now see if another common law associated with switching, that is the celebrated Merz's law³⁵, holds here or not. For that, Fig. 3 displays the logarithm of the switching time as a function of the inverse of the electric-field magnitude. Three different regimes are observed. In Regime I, which corresponds to fields smaller than $3.7 \times 10^7 \text{V/m}$, the logarithm of the switching time practically goes up vertically with the inverse of the field. On the other hand, in Regime II, that corresponds to fields ranging between $3.7 \times 10^7 \text{V/m}$

and $1.0 \times 10^8 \text{V/m}$, $\ln(t_0)$ basically linearly increases with the inverse of the fields. Such nearly linear increase is consistent with Merz's law³⁵. In Regime III, that is for fields above $1.0 \times 10^8 \text{V/m}$, the logarithm of the switching time once again deviates from a linear behavior with $1/E$. In other words, it is striking to realize that only one out of these three regimes obeys the commonly believed Merz's law³⁵!

In fact, one can understand the existence of these three regimes, and the deviation of the Merz's law for two of them, thanks to some data shown in Figs 1 and 2, especially once realizing that the fields of $3.5 \times 10^7 \text{V/m}$, $8.0 \times 10^7 \text{V/m}$ and $2.0 \times 10^8 \text{V/m}$ precisely fall into Regimes I, II and III, respectively. As a matter of fact, the switching time of Regime I is larger than the one expected from the red straight line of Fig. 3 for two reasons: for small fields, (1) the infinite cluster has a polarization along [111], whose magnitude is nearly independent on the time, for times before $t_{annih,begin}$ (see Fig. 1b); and (2) it especially takes time to break the infinite cluster in favor of rotating dipoles belonging to percolation clusters or being isolated (*cf* top of Fig. 2a). Such difficulty in breaking the infinite clusters also manifests itself into the large oscillation of both the strength of the infinite clusters and the percolation size (see top of Figs 2a and 2b), as indicative that some pieces of the infinite cluster are broken and then reattach themselves to the infinite cluster by creating and then absorbing back, respectively, some percolation clusters, for times before $t_{annih,begin}$. Other manifestations of such difficulty in breaking the infinite cluster are the large $\langle s \rangle$ occurring at $t_{annih,begin}$, as well as the large value of $t_{annih,begin}$ and the rather small ratio of $t_0/t_{annih,begin}$ (which is equal to 1.15 for the $3.5 \times 10^7 \text{V/m}$ field). Such two latter features indicate that it takes a rather long time to fully break the infinite cluster, but, then the reversal of the polarization happens relatively quickly once this infinite cluster is broken.

For intermediate fields, it takes lesser time to destroy this infinite cluster (see intermediate Fig. 2a), while the polarization of this infinite cluster remains more-or-less nearly independent on time before $t_{annih,begin}$ (*cf* Fig. 1c). In other words, the activation energy that is typically associated with the existence of a Merz's law likely concerns the energy of breaking the infinite clusters (rather than the motion of domain walls, as often assumed in the Merz's law³⁵). Note that $t_0/t_{annih,begin}$ is now equal to a larger value of 1.32 for the $8.0 \times 10^7 \text{V/m}$ field.

Finally, the switching time in Region III is much shorter than the one given by the red straight line because the polarization of the infinite cluster now decreases with time

before $t_{annih,begin}$ (as shown in Fig. 1d), while the infinite cluster continues to be more easily breakable under larger fields (see bottom of Fig. 2a). As a result, two mechanisms having two activation energies are at play here: an activation energy that is associated with the reduction of the magnitude of the polarization within the infinite clusters, and another activation energy that is inherent to the breaking of the infinite clusters. Having two different activation energies is likely the reason why the Merz's law is not applicable in Region III (since such law assumes a single activation energy). Such double activations now result in much larger $t_0/t_{annih,begin}$, i.e. of the order of 1.65 for the $2.0 \times 10^8 \text{V/m}$ field. As a result, it takes about 65% of the time to break such infinite cluster in order to bring the macroscopic polarization to zero, once the infinite cluster is broken .

IV. SUMMARY

In summary, we report here the prediction that a specific switching occurs when applying a *dc* electric field along $[\bar{1}\bar{1}\bar{1}]$ to the ferroelectric state of PMN having an initial (opposite) polarization along $[111]$. This switching is schematized in Fig. 4. It (1) first involves the progressive reduction of the number of dipoles belonging to the infinite cluster (with these dipoles lying near $[111]$), altogether with the rotations towards $[\bar{1}\bar{1}\bar{1}]$ of the dipoles being outside this infinite cluster (with these rotations resulting in a cancellation of the x' and y' components of the polarization that are perpendicular to $[111]$, unlike the z' -component that is parallel to $[111]$); is then (2) accompanied by the complete breaking of this infinite cluster in favor of a short-range, relaxor-like state inside which dipoles continue to rotate towards the field's direction (with, once again, the x' and y' directions of their dipoles canceling each other in average, while the average z' component varies from being slightly positive to slightly negative via passing through a zero at the switching time); before (3) a new infinite cluster is re-created (but inside which the dipoles are now along $[\bar{1}\bar{1}\bar{1}]$) and gains in strength, via the assimilation of finite clusters and isolated dipoles. Microscopic aspects of this switching, such as the aforementioned rotation, implies that fundamental assumptions of the standard NLS are *not* satisfied. On the other hand, the studied switching mechanism results in a polarization-*versus*-time curve that can be well fitted by the NLS model. We thus would like to propose to give another name to the presently discovered switching or to denote it as "generalized NLS model". It will also be interesting to determine, in a near future, if

the various states encountered during this polarization switching of PMN have each their own electrical resistance, and thus can form the basis of so-called memristors^{49,50}. If that is the case, some possible applications towards artificial neural networks and unsupervised learning in high-density memristive arrays¹⁸, taking advantage of the presently discovered polarization switching of PMN, may be designed (Note that polarization switching has also some consequences on elastic and related properties of the system. For instance, we numerically found (not shown here) that, for times ranging between $t_{annih,begin}$ and $t_{annih,end}$, the strain along the [111] direction typically takes its smallest values for any applied electric field). Finally, we also demonstrated that small and large applied fields result in a violation of the commonly accepted Merz's law³⁵ because of very specific local features.

We thus hope that our findings increase the current knowledge of ferroelectrics, relaxors and polarization switching, and can also be of some use for novel technologies.

S.P. and L.B. thank ONR Grants No. N00014-12-1-1034 and No. N00014-17-1-2818. B.X. acknowledges funding from Air Force Office of Scientific Research under Grant No. FA9550-16-1-0065. Some computations were also made possible owing to MRI Grant No. 0722625 from NSF, ONR Grant No. N00014-15-1-2881 (DURIP), and a Challenge grant from the Department of Defense. S.P. appreciates support of RMES 3.1649.2017/4.6. We also thank Yousra Nahas and Sergei Prokhorenko for useful discussions.

¹ J. F. Scott, *Ferroelectric memories*, **3** (Springer, 2000).

² M. Dawber, K. M. Rabe, and J. F. Scott, *Rev. Mod. Phys.* **77**, 1083 (2005).

³ V. Garcia, S. Fusil, K. Bouzehouane, S. Enouz-Vedrenne, N. D. Mathur, A. Barthelemy, and M. Bibes, *Nature* **460**, 81 (2009).

⁴ O. Lohse, M. Grossmann, U. Boettger, D. Bolten, and R. Waser, *Journal of Applied Physics* **89**, 2332 (2001).

⁵ A. Gruverman, B. J. Rodriguez, C. Dehoff, J. Waldrep, A. Kingon, R. Nemanich, and J. Cross, *Appl. Phys. Lett.* **87**, 082902 (2005).

⁶ J. Y. Jo, H. S. Han, J.-G. Yoon, T. K. Song, S.-H. Kim, and T. W. Noh, *Phys. Rev. Lett.* **99**, 267602 (2007).

⁷ D.J.Kim,J.Y.Jo,T.H.Kim,S.M.Yang,B.Chen, Y. S. Kim, and T. W. Noh, *Appl. Phys. Lett.* **91**,

- 132903 (2007).
- ⁸ S. Ducharme, V. M. Fridkin, A. V. Bune, S. P. Palto, L. M. Blinov, N. N. Petukhova, and S. G. Yudin, *Phys. Rev. Lett.* **84**, 175 (2000).
- ⁹ J. Y. Jo, D. J. Kim, Y. S. Kim, S.-B. Choe, T. K. Song, J.-G. Yoon, and T. W. Noh, *Phys. Rev. Lett.* **97**, 247602 (2006).
- ¹⁰ M. J. Highland, T. T. Fister, M.-I. Richard, D. D. Fong, P. H. Fuoss, C. Thompson, J. A. Eastman, S. K. Streiffer, and G. B. Stephenson, *Phys. Rev. Lett.* **105**, 167601 (2010).
- ¹¹ R. Gaynutdinov, M. Minnekaev, S. Mitko, A. Tolstikhina, A. Zenkevich, S. Ducharme, and V. Fridkin, *Physica B* **424**, **8** (2013).
- ¹² Y.-H. Shin, I. Grinberg, I.-W. Chen, and A. M. Rappe, *Nature* **449**, 881 (2007).
- ¹³ S. Liu, I. Grinberg, and A. M. Rappe, *Appl. Phys. Lett.* **103**, 232907 (2013).
- ¹⁴ S. Liu, I. Grinberg, and A. M. Rappe, *Nature* **534**, 360 (2016).
- ¹⁵ A. K. Tagantsev, I. Stolichnov, N. Setter, J. S. Cross, and M. Tsukada, *Phys. Rev. B* **66**, 214109 (2002).
- ¹⁶ R. Xu, S. Liu, I. Grinberg, J. Karthik, A. R. Damodaran, A. M. Rappe, and L. W. Martin, *Nat. Mater.* **14**, 79 (2015).
- ¹⁷ B. Xu, V. Garcia, S. Fusil, M. Bibes, and L. Bellaiche, *Phys. Rev. B* **95**, 104104 (2017).
- ¹⁸ S. Boyn *et al.*, *Nat. Commun.* **8**, 14736 (2017).
- ¹⁹ A. N. Kolmogorov, *Izv. Akad. Nauk, Ser. Math.* **1**, 355 (1937).
- ²⁰ M. Avrami, *J. Chem. Phys.* **8**, 212 (1940).
- ²¹ Y. Ishibashi and Y. Takagi, *J. Phys. Soc. Jpn.* **31**, 506 (1971).
- ²² S. Bhattacharjee, D. Rahmedov, D. Wang, J. Íñiguez and L. Bellaiche, *Phys. Rev. Lett.* **112**, 147601 (2014).
- ²³ S. H. Baek and C. B. Eom, *Phil. Trans. R. Soc. A* **370**, 4872 (2012).
- ²⁴ L. E. Cross, *Ferroelectrics* **151**, 305 (1994).
- ²⁵ G. A. Smolensky *et al.*, *Ferroelectrics and Related Materials*, (Gordon and Breach, New York 1981).
- ²⁶ D. Viehland, S. J. Jang, L. E. Cross and M. Wuttig, *J. Appl. Phys.* **68**, 2916 (1990).
- ²⁷ G. Burns and F. H. Dacol, *Phys. Rev. B* **28**, 2527 (1983).
- ²⁸ R. Blinc, V. V. Laguta, and B. Zalar, *Phys. Rev. Lett.* **91** 247601 (2003).
- ²⁹ B. Dkhil, J. M. Kiat, G. Calvarin, G. Baldinozzi, S. B. Vakhrushev, and E. Suard, *Phys. Rev.*

- B **65**, 024104 (2001).
- ³⁰ P. M. Gehring, S. Wakimoto, Z. G. Ye, and G. Shirane, Phys. Rev. Lett. **87**, 277601 (2001).
- ³¹ Z. Kutnjak, B. Vodopivec, and R. Blinc, Phys. Rev. B **77**, 054102 (2008).
- ³² X. Zhao, W. Qu, X. Tan, A. A. Bokov, and Z.-G. Ye, Phys. Rev. B **75**, 104106 (2007).
- ³³ Z. Kutnjak, R. Blinc, and Y. Ishibashi, Phys. Rev. B **76**, 104102 (2007).
- ³⁴ E. V. Colla, E. Yu. Koroleva, N. M. Okuneva, and S. B. Vakhrushev, Phys. Rev. Lett. **74**, 1681 (1995).
- ³⁵ W. J. Merz, Phys. Rev. **95**, 690 (1954).
- ³⁶ D. C. Rapaport, The Art of Molecular Dynamics Simulation. Cambridge University Press: New York, 1996.
- ³⁷ A. Al-Barakaty, S. Prosandeev, D. Wang, B. Dkhil, and L. Bellaiche, Phys. Rev. B **91** 214117 (2015).
- ³⁸ W. Zhong, D. Vanderbilt, and K. M. Rabe, Phys. Rev. Lett. **73**, 1861 (1994).
- ³⁹ S. Prosandeev and L. Bellaiche, Phys. Rev. B **94**, 180102(R) (2016).
- ⁴⁰ H. Taniguchi, M. Itoh and D. Fu, J. Raman Spectrosc. **42**, 706 (2011).
- ⁴¹ S. Wakimoto, C. Stock, R. J. Birgeneau, Z.-G. Ye, W. Chen, W. J. L. Buyers, P. M. Gehring, and G. Shirane, Phys. Rev. B **65**, 172105 (2002).
- ⁴² A. Al-Zein, J. Hlinka, J. Rouquette, and B. Hehlen, Phys. Rev. Lett. **105**, 017601 (2010).
- ⁴³ B. Hehlen, M. Al-Sabbagh, A. Al-Zein, and J. Hlinka, Phys. Rev. Lett. **117**, 155501 (2016).
- ⁴⁴ V. Bovtun, S. Veljko, S. Kamba, J. Petzelt, S. Vakhrushev, Y. Yakymenko, K. Brinkman, N. Setter, J. Europ. Ceram. Soc. **26**, 2867 (2006).
- ⁴⁵ Z. Jiang, Y. Nahas, S. Prokhorenko, S. Prosandeev, D. Wang, J. Íñiguez, and L. Bellaiche, Phys. Rev. B **97**, 104110 (2018).
- ⁴⁶ Z. Jiang, S. Prokhorenko, S. Prosandeev, Y. Nahas, D. Wang, J. Íñiguez, E. Defay, and L. Bellaiche, Phys. Rev. B **96**, 014114 (2017).
- ⁴⁷ B. Xu, J. Íñiguez, and L. Bellaiche, Nat. Commun. **8**, 15682 (2017).
- ⁴⁸ Dietrich Stauffer and Amnon Aharony. Introduction to Percolation Theory. CRC Press, 2nd edition, 1994.
- ⁴⁹ J. J. Yang, D. B. Strukov, and D. R. Stewart, Nat. Nanotechnol. **8**, 13 (2013).
- ⁵⁰ L. O. Chua, IEEE Trans. Circuit Theory **18**, 507 (1971).

CAPTIONS.

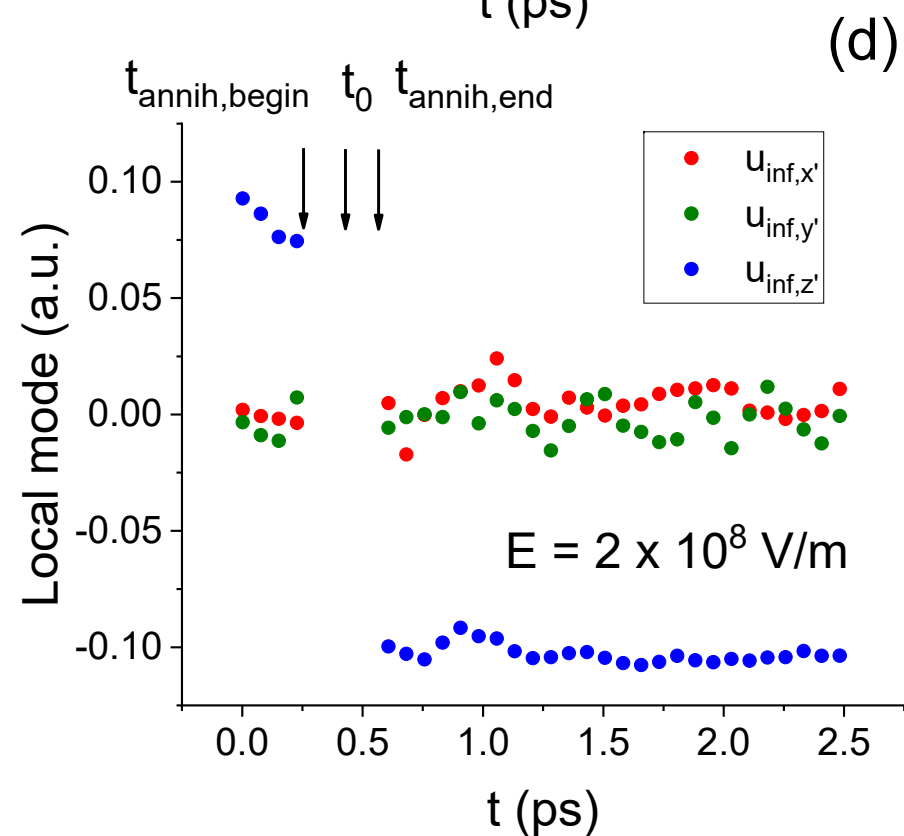
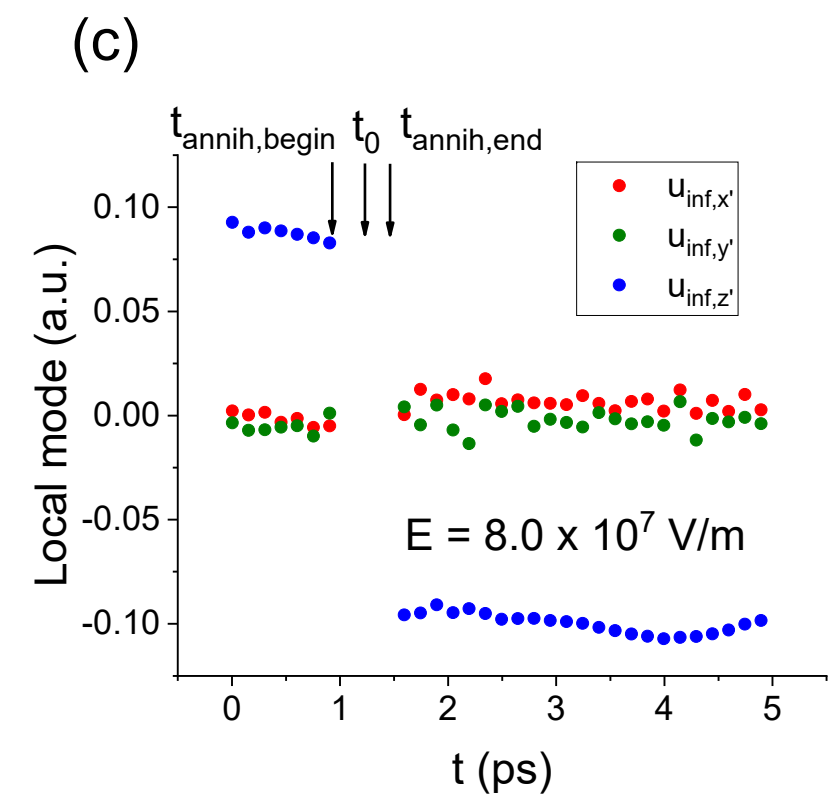
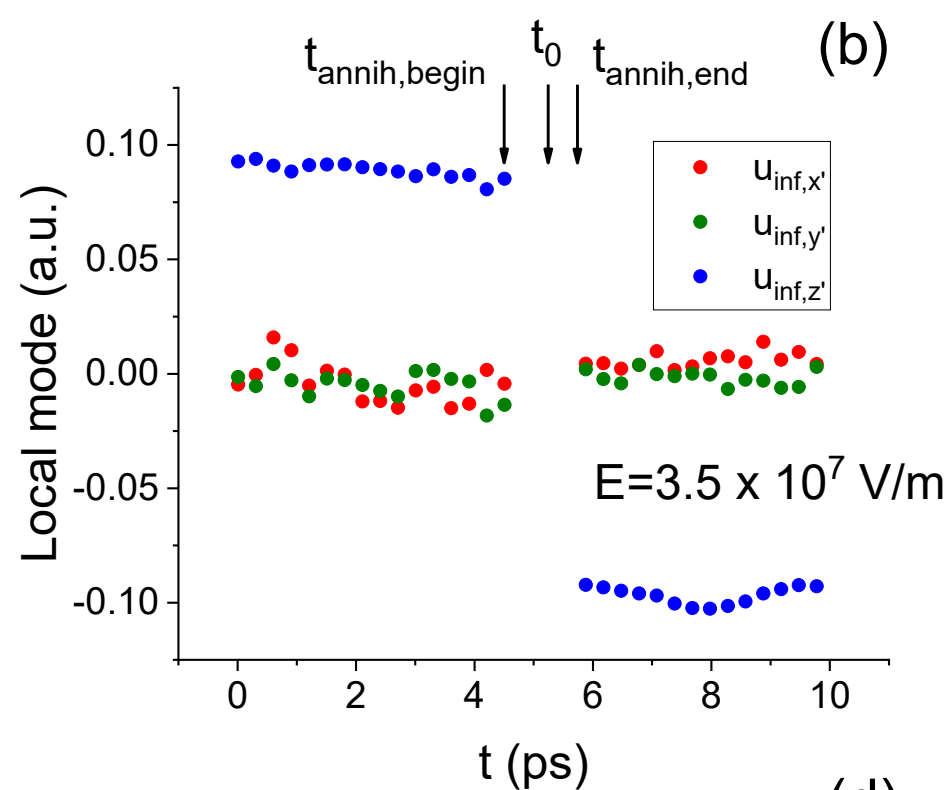
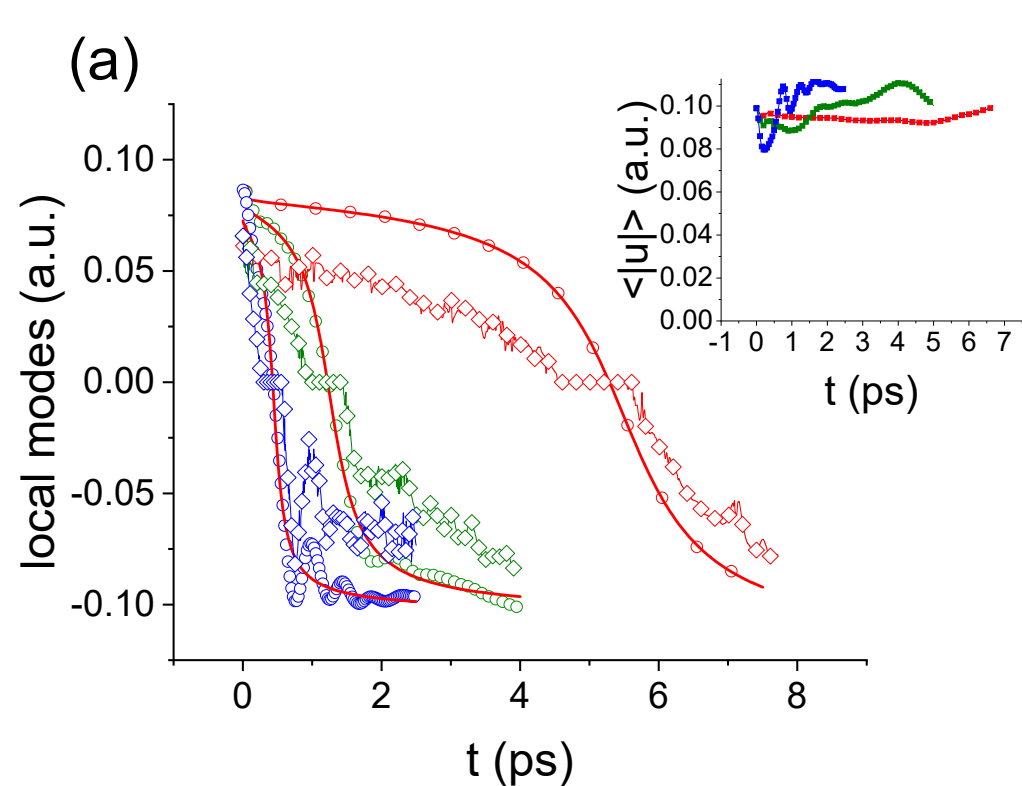
Figure 1 (color online). Local modes as a function of time. Panel (a) shows the temporal dependence of the $\langle \mathbf{u} \rangle$ supercell average of the local mode vectors for three different external electric fields applied along the $[\bar{1}\bar{1}\bar{1}]$ direction. These three electric fields have a magnitude of $3.5 \times 10^7 \text{V/m}$, $8.0 \times 10^7 \text{V/m}$ and $2.0 \times 10^8 \text{V/m}$, respectively, and correspond to the use of red, green and blue colors, respectively. Only the z' -component of $\langle \mathbf{u} \rangle$ is shown (by means of open circles), because its x' and y' -components are basically null at any time and field. The thick red solid lines represent fit of the MD data for this z' -component of $\langle \mathbf{u} \rangle$ by the NLS model. Moreover, the product of P_{inf} and $u_{inf,z}$ (see text) is also displayed by means of open rhombus in Panel a, and the $\langle |u| \rangle$ average magnitude of the individual local modes is further shown in the inset of Panel (a) (via filled squares). Panels (b), (c) and (d) represent the x' , y' and z' components of the averaged local mode of the infinite cluster as a function of time, for electric fields of 3.5×10^7 , 8.0×10^7 , and $2.0 \times 10^8 \text{V/m}$, respectively. The arrows show the positions of $t_{annih,begin}$, t_0 , and $t_{annih,end}$. Note that there are no data in Panels (b), (c) and (d) for times ranging between $t_{annih,begin}$ and $t_{annih,end}$, simply because there is no infinite cluster during this time interval.

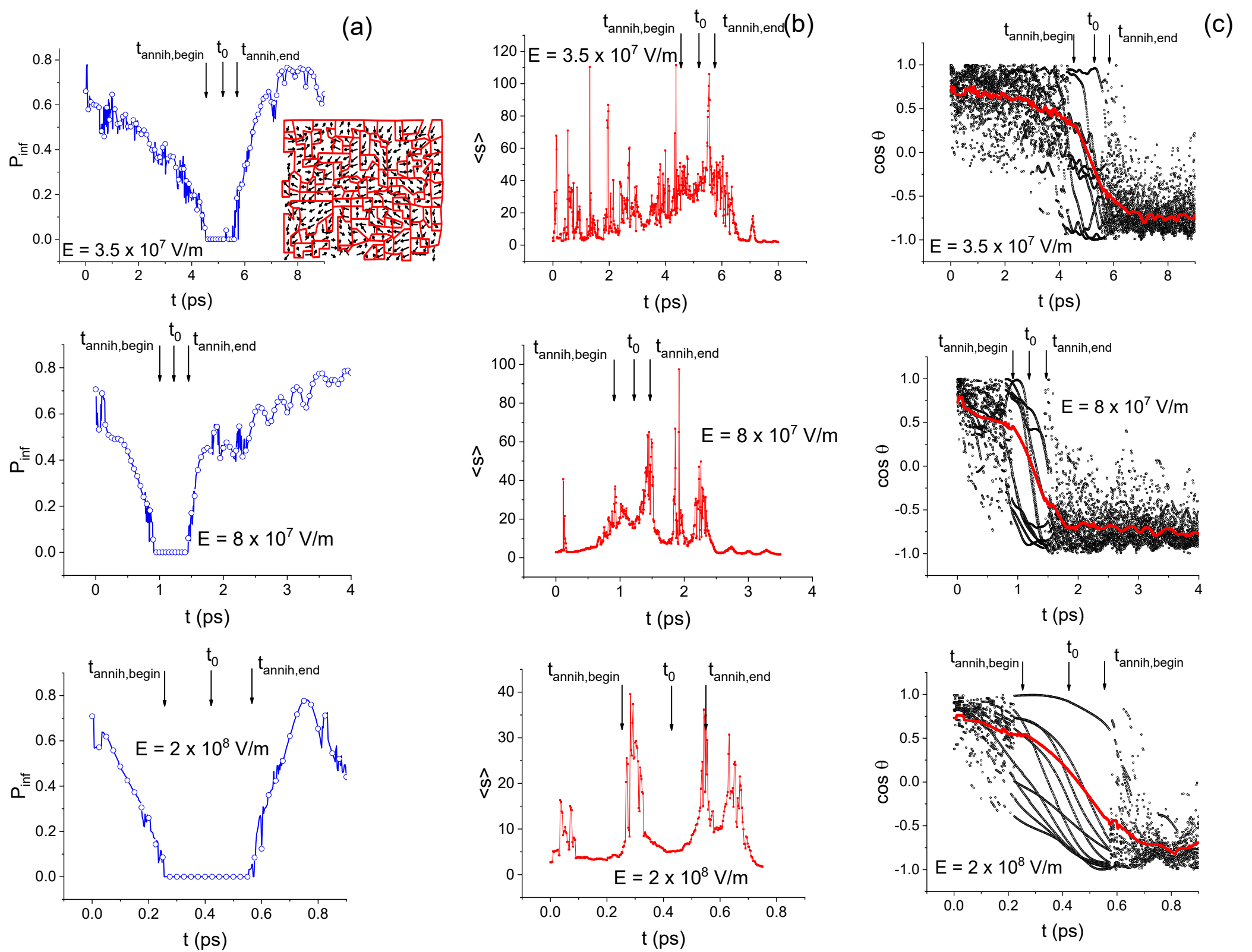
Figure 2 (color online). Temporal dependence of some local quantities for the three different dc fields indicated in Fig. 1, namely of $3.5 \times 10^7 \text{V/m}$, $8.0 \times 10^7 \text{V/m}$ and $2.0 \times 10^8 \text{V/m}$'s magnitude, for the top, intermediate and bottom panels, respectively. Panels (a), (b), and (c) display the strength of the infinite cluster, percolation cluster size, and $\cos(\theta)$ (see text), respectively. The inset in the top of Panel (a) represents a snapshot of the dipole pattern at time t_0 for the applied field of $3.5 \times 10^7 \text{V/m}$, with red colors delimiting the percolation clusters (that coincide with polar nanoregions). The red thick line of Panel (c) display $\langle \cos(\theta) \rangle_{not\ inf}$ (see text too). The arrows in all panels show the positions of $t_{annih,begin}$, t_0 , and $t_{annih,end}$.

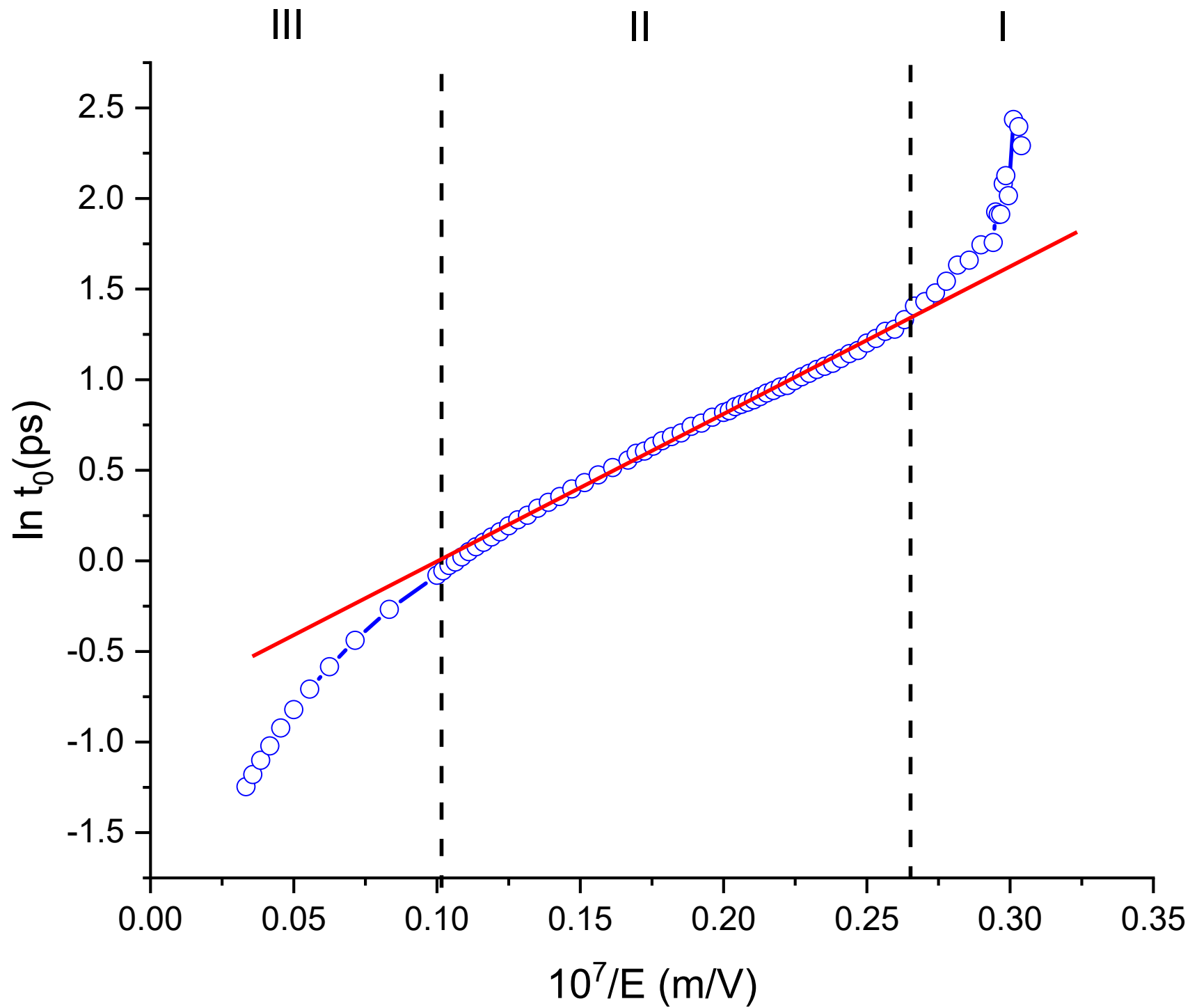
Figure 3 (color online). Dependence of the logarithm of the t_0 switching time on the inverse magnitude of the applied electric field. The dashed vertical lines delimit the Regions I, II and III indicated in the text, while the red solid line represents a linear fit of the data in Region II.

Figure 4 (color online). Schematization of the studied switching mechanism. Panel (a) emphasizes that, in the initial stage of switching, the infinite cluster has dipoles along $[111]$ and coexists with finite percolation clusters having dipoles in directions being different from

$[111]$, but so that their average is also along $[111]$. Small percolation clusters in this stage have therefore x' - and y' -components of dipoles being perpendicular to $[111]$, but that vanish after averaging out over all percolation clusters. Panel (b) indicates that the infinite cluster is reduced in terms of relative number of dipoles, and that the dipoles belonging to the percolation clusters are rotating towards $[\bar{1}\bar{1}\bar{1}]$, while still maintaining their overall averaged x' - and y' - components equal to zero. Panel (c) shows that, at $t = t_0$, there is no more infinite cluster, while the dipoles in the percolating clusters fully cancel their polarization on average along any direction (as consistent with the inset of the top of Fig. 2a); Panel (d) emphasizes the reappearance of the infinite cluster, with dipoles being along $[\bar{1}\bar{1}\bar{1}]$ now, and the dipoles of the percolating clusters having now directions getting closer to $[\bar{1}\bar{1}\bar{1}]$ but still canceling each other their x' - and y' -components (unlike their z' -component that is now negative). Finally, Panel (e) can be thought as the reciprocal situation of Panel (a), in the sense that there is a large infinite cluster, but with polarization along $[\bar{1}\bar{1}\bar{1}]$ that coexists with a few percolating clusters whose dipoles deviate from $[\bar{1}\bar{1}\bar{1}]$ but for which their x' - and y' -components cancel each other while their average z' -component is negative.

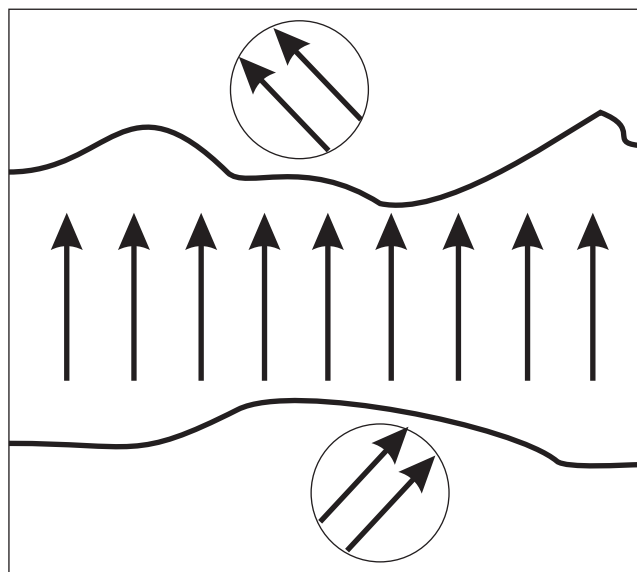




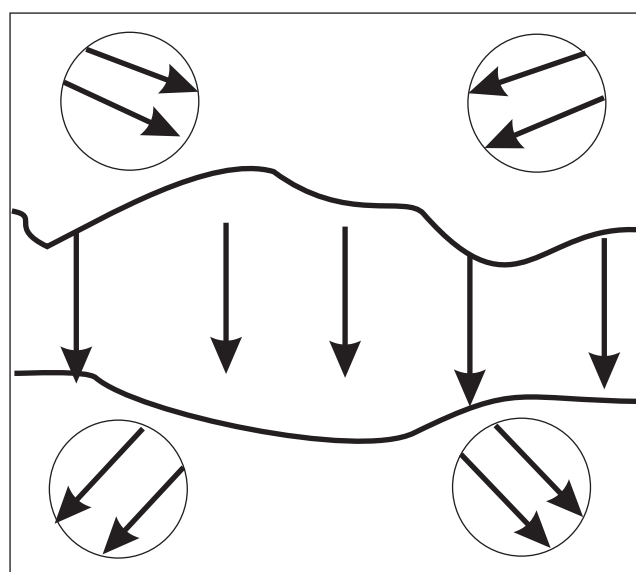


[111]

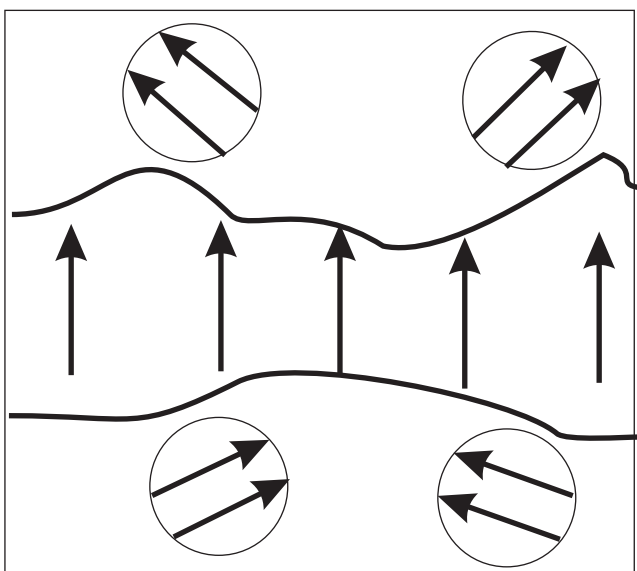
(a)



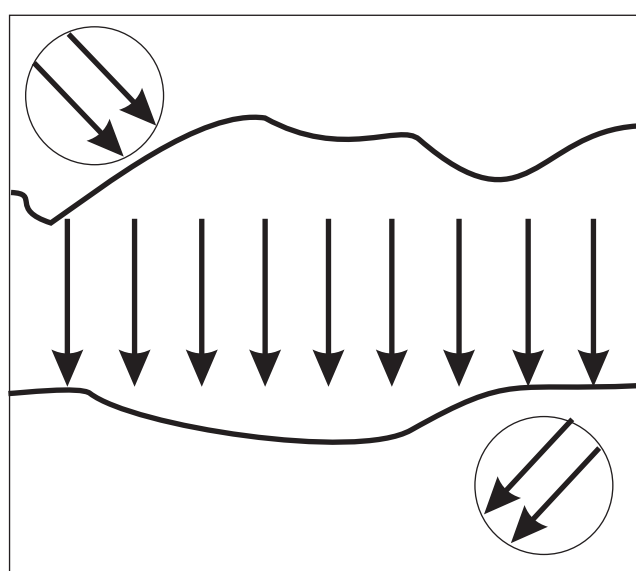
(d)



(b)



(e)



(c)

